

# Uncertainty propagation for the assessment of tumoral masses segmentation

Arianna Mencattini, Giulia Rabottino, and Marcello Salmeri  
Dept. Electronic Engineering  
University of Rome, “Tor Vergata”, Rome, Italy  
Email: mencattini,rabottino,salmeri@ing.uniroma2.it

Simona Salicone  
Dip. Elettrotecnica  
Politecnico di Milano, Italy  
Email: simona.salicone@polimi.it

**Abstract**—In this paper we perform the assessment of a tumoral mass segmentation and characterization algorithm by implementing the uncertainty propagation through the blocks. We use a Monte Carlo method owing to the iterative and very complex structure of the algorithms used. The validation of the results is based on confidence intervals for given coverage probabilities and ad hoc performance metrics.

## I. INTRODUCTION

Breast cancer is the second cause of cancer death among women in the world. Mostly, this is motivated by the fact that 10% – 15% of tumors are missed on mammography. Two kinds of mistakes can be done: in the visual search (30% of failures) and in the interpretation (70% of failures). The former are perceptual errors (insufficient time of observation for the correct recognition of the lesion) and the latter are decision-making errors (the lesion is detected but an incorrect decision is made).

Cancer signs are microcalcifications in the early stage and massive lesions when the cancer is grown. Microcalcifications are small bright spots often clustered with a mean diameter in the range  $[0.1 - 1]$  mm, whereas tumoral masses are space occupying lesions (mean diameter of  $[10 - 400]$  mm), with a very low contrast, ill-defined margins, and luminance characteristics similar to the fatty glandular tissue. Both signs are difficult to be detected.

An optimal situation for the early diagnosis of breast cancer would be to have two expert radiologists acting as first and second readers that independently observe the mammographic image and determine if there is a suspicious region to be investigated. This procedure is expensive, complex and time consuming especially in screening programs where a huge number of mammographic images have to be read.

The development of computerized systems as second readers is an alternative. Researchers have been investigating algorithms to detect mammographic abnormalities for more than 30 years with the aim of automating mammographic interpretation [1]. Computer-aided detection (CADe) and diagnosis (CADx) systems are widely used in mammography, where signs of early breast cancer are often very subtle. CAD involves the use of computer algorithms to detect patterns in images associated with signs of disease.

In a recent literature, we have presented the metrological assessment of different blocks of a new and complex CADx

system, dealing with the enhancement and denoising step of the mammographic images [2], [3] and with the microcalcifications segmentation and characterization step [4]. In [5] we have preliminarily investigated the metrics needed to evaluate the performance of a mass segmentation block. So, in this paper we provide a full metrological validation of the mass segmentation algorithm able to extract shape and margins of tumoral masses with the aim of classifying them as benign or malignant. The assessment is performed by uncertainty propagation through the whole system concerning both the segmentation step and the features extraction procedure.

## II. MASS SEGMENTATION AND FEATURES EXTRACTION

Tumoral mass segmentation is a critical step owing to the nature of the lesions to be detected. In fact, the masses shape can be round, oval, lobular, or irregular and margins can be circumscribed, microlobulated, obscured, indistinct, or spiculated. Moreover, masses have a very low-contrast with a luminance that usually decreases as the distance from the center of the lesion increases. Normal glandular tissue has luminance characteristics very similar to the mass and the boundary of the mass appears to be blurred owing to scattering, noise and similar absorption characteristics between the mass and the tissue surrounding it. For these reasons, region-based algorithms appear to be the most effective methods in this context, since they simultaneously use intensity, spatial and connectivity information to identify boundary pixels.

A detailed description of the region-growing algorithm we apply can be found in [5], [6]. Here we only recall the fundamental steps of the whole segmentation procedure including a preliminary enhancement step and a region-growing block so that the reader can better understand the uncertainty propagation flow.

- ◊ A Region Of Interest (ROI) is preliminarily manually extracted by the radiologist. At the moment, a procedure for the automatic detection of suspicious regions of interest is under consideration but it is beyond the scope of this work.
- ◊ Artifacts are removed from the image by a pixel-based automatic procedure. This step is fundamental since artifacts can be considered as part of the mass boundary thus altering its geometry.

- ◇ Contrast is improved in the ROI in order to increase the luminance difference between the mass and the neighboring pixels belonging to the normal tissue. Denoting with  $I(n, m)$  the luminance in the original low contrast ROI, then the luminance in the enhanced ROI is given by

$$I_E(n, m) = \left( \frac{I(n, m)}{\max(I(n, m))} \right)^4$$

The preliminary normalization is needed so that the global image with a luminance in the range  $[0, 1]$  does not darken.

- ◇ A multitolerance one-seed region-growing algorithm [6], [5] is applied to  $I_E(n, m)$  so that a region is grown around a seed pixel that is manually chosen approximately at the center of the mass. Actually, this choice does not strongly affect the final result since the luminance of the seed is always chosen as the mean luminance of a  $15 \times 15$  region around the seed. This operation is also reapplied inside the algorithm so that the robustness to noise is also increased. As fully described in [5], [6] the algorithm we apply is also optimized since a preliminary decimation is performed on the ROI to extract a rough mass boundary. Then, the contour is refined by running the region-growing algorithm choosing as seeds pixels belonging to the rough boundary preliminarily extracted.

After the ROI has been segmented, a binary mask containing the mass region only is achieved and applied to the original ROI. Some examples are shown in Fig. 1<sup>1</sup>. Then, for each

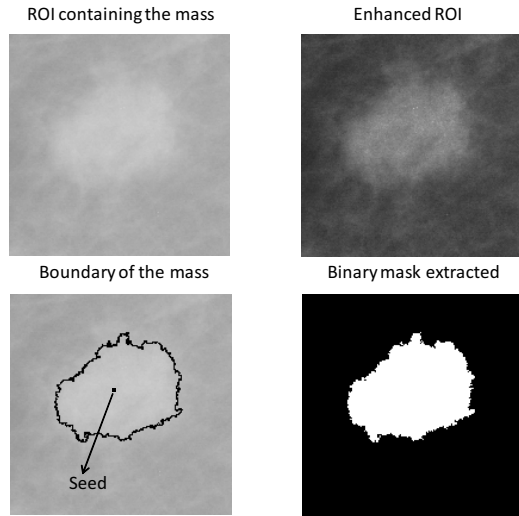


Fig. 1. Original ROI with a mass (up-left), enhanced ROI (up-right), boundary extracted for the tumoral mass (bottom-left) and the derived binary mask (bottom-right).

segmented mass a set of features are evaluated in order to assign a malignancy index to it. As a preliminary investigation

<sup>1</sup>The image is taken from Digital Database for Screening Mammography (DDSM) [7] containing more than 4000 12 bpp mammographic images with a spatial resolution of  $40 \mu\text{m}$

here we only consider shape features while in the final paper we will also concern textural features. The first ones take into account only geometrical aspects of the boundary while the second ones consider also the internal structure of the mass. In fact, benign and malignant masses often differ for imperceptible and subtle details, so that a large set of parameters have to be considered simultaneously.

In particular, here we compute the following parameters whose graphical description is reported in Fig. 2:

- Area of the segmented mass  $f_1$ .
- Perimeter of the boundary of the segmented mass  $f_2$ .
- Statistical parameters of the radius of the segmented mass with respect to its centroid (mean  $f_3$ , standard deviation  $f_4$ , skewness  $f_5$ , kurtosis  $f_6$ ).
- Circularity of the segmented mass boundary  $f_7 = (f_2)^2 / (f_1 \cdot 4\pi)$ .
- Eccentricity of the segmented mass boundary  $f_8$ .
- Entropy of the segmented mass  $f_9$  which actually is the only not geometrical parameter. It is given by  $-\sum_{(n,m)} (I(n, m) \cdot \log(I(n, m)))$
- Rectangularity of the segmented mass boundary  $f_{10} = \text{Area}(\text{BOUNDING BOX}) / f_1$ .
- Boundary Roughness of the segmented mass boundary  $f_{11}$  related to the gradient of the radius.
- Zero Crossing of the segmented mass boundary  $f_{12}$ .

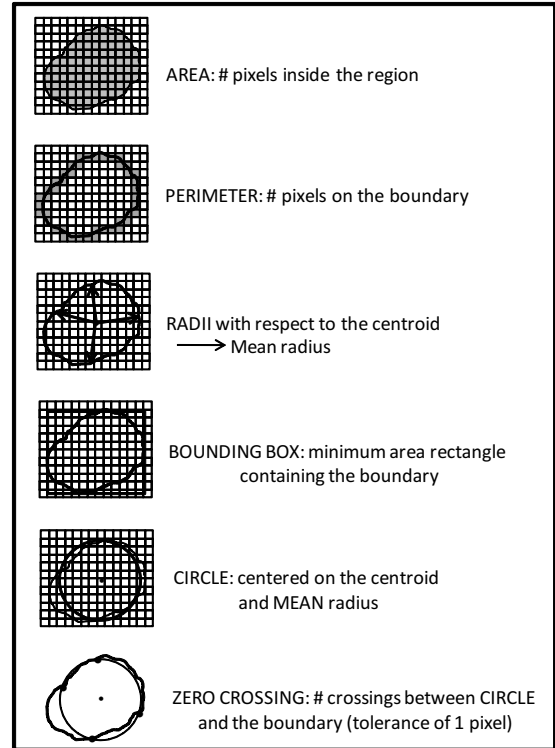


Fig. 2. Graphical description of some features.

These parameters are crucial in order to classify tumoral masses into benign and malignant ones. So, the uncertainty contribution associated to each of them, due to the uncertainty

in the pixel intensity value, is a critical aspect that should be taken into account in the classification step.

### III. UNCERTAINTY PROPAGATION

Uncertainty propagation is performed in this paper by a Monte Carlo simulation. This choice is motivated by two main reasons:

- the random nature of effects we assume affecting the pixel luminance in the image, mostly due to noise, allows us to perform a Monte Carlo simulation in order to propagate this contribution through the region-growing algorithm and features evaluation steps;
- the iterative structure of the region-growing algorithm makes unsuitable other kinds of uncertainty propagation methods in this preliminary investigation;

Following recommendations in [8] we work as follows.

- i) Represent the luminance of each pixel by a normal random variable [2] with mean value the given luminance value and standard deviation obtained by a preliminary noise variance estimation performed on the whole image [9], [10]. As already noted [2], [10] noise in mammographic images is heteroscedastic so that its variance depends on the pixel intensity values.
- ii) Generate a sample luminance value for each pixel in a selected ROI from the distribution assumed at step i).
- iii) Apply the region-growing algorithm to the generated image until its stopping criteria is verified.
- iv) Evaluate parameters described above on the boundary extracted at step iii).
- v) Repeat steps ii) - v)  $M$  times. In our case, owing to the huge dimension of the ROI containing the mass (about  $1000 \times 1000$  pixels, we choose  $M = 100$ . Since each iteration takes about 10 s, the whole simulation takes 20 minutes.

At the end of steps i)-v) we obtain a set of values for each parameter and a boundary region given by the difference between the union of all the internal regions inside the boundaries selected and the intersection among them. The boundary region we obtain can be easily understood considering Fig. 3. In fact, suppose that the region-growing algorithm has been

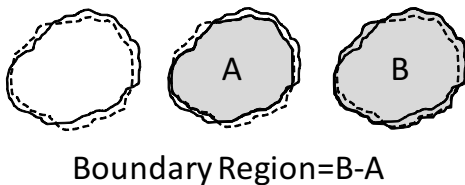


Fig. 3. Boundary region derived from two different boundaries.

run two times thus producing the two boundaries shown in Fig. 3 by the solid and the dashed lines respectively. Denote the two boundaries with  $b_1$  and  $b_2$  and with  $B_1$  and  $B_2$  the regions having  $b_1$  and  $b_2$  as boundaries. Then we get that

$$A = B_1 \cap B_2, \quad B = B_1 \cup B_2$$

Finally, the Boundary Region is given by  $B - A$ . This region identifies the global uncertainty associated to the boundary extracted by the region-growing algorithm since it directly derives from the variation of the pixel intensity values in the selected ROI.

### IV. VALIDATION OF THE RESULTS

Two kinds of validation methods can be applied at the end of the uncertainty propagation.

Regarding the boundary region we need to compare it with a reference boundary, called ground-truth in the medical context [11], provided by an expert radiologist by hand. Then, as described in [5], we compute two indexes called *Correctness* (CR) and *Completeness* (CM) given by

$$CR = \frac{TP}{TP + FP}, \quad CM = \frac{TN}{TN + FN}$$

where  $TP$ ,  $TN$ ,  $FP$ , and  $FN$  are the *True Positives*, *True Negatives*, *False Positives*, and *False Negatives* pixels. Commonly, the comparison is between a *single boundary* extracted from an algorithm and a reference one, while in this context the comparison is between a *boundary region* and the reference contour. In the final paper we will provide quantitative results concerning this kind of assessment.

Regarding the features extracted for the classification of the masses, we build for each of them a Cumulative Distribution Function (CDF) so that, following [8] we can evaluate a coverage interval for a given coverage probability for each features extracted. Also, the mean value of each feature is evaluated as a reference value.

This characterization will be crucial in the classification procedure, allowing us to assign a weight to the features used. As an example, the CDF and the histograms obtained for features  $f_1$  and  $f_4$ , for a coverage probability  $p = 0.9$ , are shown in Fig. 4. Table I shows the confidence intervals obtained for the 12 parameters  $f_1 - f_{12}$  with coverage probabilities  $p = \{0.5, 0.75, 0.9, 0.95, 0.99\}$ . Also the reference value is provided below the feature name.

### V. FUTURE DEVELOPMENTS

In the final paper we will address the following items:

- ◇ Uncertainty representation of the pixel luminance could be refined taking into account, if needed, not random contributions. A recent literature [12] has pioneered this argument. As a consequence, alternative approaches for the uncertainty propagation should be considered and compared.
- ◇ The assessment of the whole segmentation algorithm will be accomplished also providing quantitative results for the correctness and completeness indexes.
- ◇ Confidence intervals for the textural features will be also provided thus identifying a complete set of parameters for the classification of tumoral masses.
- ◇ The segmentation procedure will be speeded up, so that a larger  $M$  could be chosen in the Monte Carlo simulation.

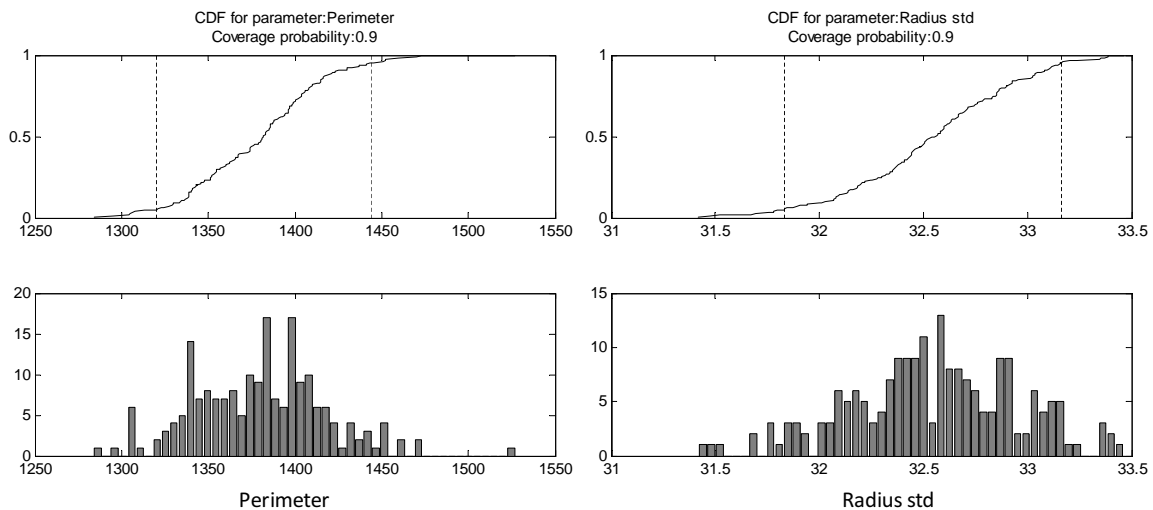


Fig. 4. Histograms and CDF for perimeter and std of radius.

TABLE I

CONFIDENCE INTERVALS FOR THE 12 FEATURES COMPUTED FOR EACH BOUNDARY WITH COVERAGE PROBABILITIES [0.5, 0.75, 0.9, 0.95, 0.99].

p \ features	$f_1$	$f_2$	$f_3$	$f_4$	$f_5$	$f_6$	$f_7$	$f_8$	$f_9$	$f_{10}$	$f_{11}$	$f_{12}$
	46824	1380	126	32.5	0.079	1.74	3.24	-2.73	0.735	5.23	277	32.2
0.5	145.5	52.0	1.1	0.55	0.040	0.048	0.236	0.047	0.019	0.067	6.0	5.06
0.75	252.0	79.5	1.7	0.95	0.070	0.077	0.360	0.079	0.031	0.119	10.0	8.93
0.9	365.0	123.5	2.6	1.33	0.104	0.103	0.585	0.115	0.043	0.178	14.0	13.69
0.95	464.5	150.5	3.2	1.62	0.127	0.124	0.701	0.134	0.054	0.215	15.5	16.32
0.99	1051.5	210.5	4.2	1.98	0.183	0.170	0.981	0.168	0.066	0.350	19.5	22.00

## VI. CONCLUSIONS

In this paper we have present some preliminary results regarding the uncertainty propagation through a tumoral mass segmentation algorithm applied in the context of mammographic images. The system we implement includes an enhancement procedure, a region-growing algorithm for the extraction of the mass boundary and finally a features extraction step in needed for the classification of the identified mass. The whole block represents the final step of a CADx system able to assist the radiologist in the early diagnosis of breast cancer.

## REFERENCES

- [1] M. Bazzocchi, F. Mazzarella, C. Del Frate, R. Girometti, and C. Zuiani, "CAD systems for mammography: a real opportunity? a review of the literature," *La Radiologia Medica*, vol. 112, no. 3, pp. 329 – 353, Apr 2007.
- [2] A. Mencattini, G. Rabottino, S. Salicone, and M. Salmeri, "Uncertainty handling and propagation in x-ray images analysis systems by means of random fuzzy variables," in *IEEE International Workshop on Advanced Methods for Uncertainty Estimation in Measurement (AMUEM '08)*, Sardinia, Trento, Italy, July 2008.
- [3] A. Mencattini, G. Rabottino, S. Salicone, and M. Salmeri, "Uncertainty modeling and propagation through rfv's for the assessment of cadx systems in digital mammography," submitted.
- [4] A. Mencattini, G. Rabottino, M. Salmeri, F. Caselli, and R. Lojacono, "Features extraction for microcalcification clusters classification in digital mammograms," in *IMEKO TC4 Symposium (IMEKOTC4 '08)*, Firenze, Italy, Sep 2008.
- [5] G. Rabottino, A. Mencattini, M. Salmeri, F. Caselli, and R. Lojacono, "Mass contour extraction in mammographic images for breast cancer identification," in *IMEKO TC4 Symposium (IMEKOTC4 '08)*, Firenze, Italy, Sep 2008.
- [6] A. Mencattini, G. Rabottino, M. Salmeri, R. Lojacono, and E. Colini, "Breast mass segmentation in mammographic images by an effective region growing algorithm," *Lecture Notes on Computer Science (Springer-Verlag)*, vol. 5259, pp. 948–957, October 2008.
- [7] University of South Florida, "University of south florida digital mammography home page," 2000, <http://marathon.csee.usf.edu/Mammography/Database.html>.
- [8] "Evaluation of measurement data - Supplement 1 to the "guide to the expression of uncertainty in measurement" - propagation of distributions using a Monte Carlo method," Tech. Rep., 2008, [http://www.bipm.org/utls/common/documents/jcgm/JCGM\\_101\\_2008\\_E.pdf](http://www.bipm.org/utls/common/documents/jcgm/JCGM_101_2008_E.pdf).20080623.
- [9] P. Gravel, B. Gilles, and J. A. De Guise, "A method for modeling noise in medical images," *IEEE Trans. Med. Imag.*, vol. 23, no. 10, pp. 1221 – 1232, Oct 2004.
- [10] M. Salmeri, A. Mencattini, G. Rabottino, and R. Lojacono, "Signal-dependent noise characterization for mammographic images denoising," in *IMEKO TC4 Symposium (IMEKOTC4 '08)*, Firenze, Italy, Sep 2008.
- [11] M. A. Wirth, *Performance Evaluation of CADE Algorithms in mammography*, chapter Recent advances in breast imaging, mammography, and computer aided diagnosis of breast cancer, pp. 639 – 699, SPIE Press, Washington, USA, 2006.
- [12] A. Mencattini and S. Salicone, "A comparison between different methods for processing the random part of random-fuzzy variables representing measurement results," in *IEEE International Workshop on Advanced Methods for Uncertainty Estimation in Measurement (AMUEM '08)*, Sardinia, Trento, Italy, July 2008.